C. elegans Body Wall Muscles are Simple Actuators

Jordan H. Boyle [a] and Netta Cohen [a,b]

[a] *School of Computing, University of Leeds, Leeds LS2 9JT, UK*
[b] *Institute of Membrane and Systems Biology, University of Leeds, Leeds LS2 9JT, UK*

Abstract

Over the past four decades, one of the simplest nervous systems across the animal kingdom, that of the nematode worm *C. elegans*, has drawn increasing attention. This system is the subject of an intensive concerted effort to understand the behaviour of an entire living animal, from the bottom up and the top down. *C. elegans* locomotion, in particular, has been the subject of a number of models, but there is as yet no general agreement about the key (rhythm generating) elements. In this paper we investigate the role of one component of the locomotion subsystem, namely the body wall muscles, with a focus on the role of inter-muscular gap junctions. We construct a detailed electrophysiological model which suggests that these muscles function, to a first approximation, as mere actuators and have no obvious rhythm generating role. Furthermore, we show that within our model inter-muscular coupling is too weak to have a significant electrical effect. These results rule out muscles as key generators of locomotion, pointing instead to neural activity patterns. More specifically, the results imply that the reduced locomotion velocity observed in unc-9 mutants is likely to be due to reduced neuronal rather than inter-muscular coupling.

Key words: *Caenorhabditis elegans* locomotion, body wall muscles, gap junctions, conductance based models

1. Introduction

Over more than a century, huge advances have been made in understanding the operation of neurons at a cellular and sub-cellular level, as well as in abstractly understanding the operation of large scale neural networks, such as those found in mammalian cortex. However, despite these impressive advances, we have yet to succeed in fully understanding the neural basis of all but the simplest behaviours. One organism, *Caenorhabditis elegans*, provides us with the first tangible possibility of understanding complex behaviours of an organism from the genetic and molecular level, through the cellular level, right up to the system level (and back down).

C. elegans is a small (about 1mm long) nematode worm [1], which has been the subject of much scientific research over the years. It is extensively used as a model organism for genetic research, due in part to its short life cycle and fully sequenced genome [2]. In addition, it is an attractive subject for research on the neural basis of behaviour due to an invariant nervous system consisting of a mere 302 neurons in the adult hermaphrodite. While the connectivity of its nervous system is known to an unprecedented degree of accuracy, far less information is available on the electrical properties of these neurons. Thus the question of the neural basis of *C. elegans* behaviour is still an open and attractive one.

Models of *C. elegans* locomotion generally focus on the worm's nervous system [3–5] or body mechanics [6,7], but there is reason to believe the participation of body wall muscles in locomotion may extend beyond their role as actuators. One of the main reasons for this hypothesis is that the muscles are electrically coupled to each other by gap junc-

Email address: netta@comp.leeds.ac.uk (Netta Cohen).

tions which, when defective, lead to a phenotype of impaired locomotion.

In this paper, we rely on electrophysiological data recorded from body wall muscles in acutely dissected preparations to construct a model of individual and coupled muscle cells. We then use this model to determine what possible active role may be attributed to individual *C. elegans* body wall muscles and, furthermore, to determine the consistency of such a model with the observed phenotype of gap junction defective worms. More specifically, we attempt to address the following questions: Do the muscles typically fire action potentials? What is their contribution to the generation of rhythmic behaviour? And finally, how strong is the inter-muscular coupling, and to what extent does it affect locomotion?

2. Background

2.1. *C. elegans locomotion*

C. elegans movement on a firm substrate typically consists of periods of forward crawling interspersed with short periods of backward crawling and turns. Forwards and backwards locomotion are achieved by propagating sinusoidal undulations along the body from head to tail (or tail to head). The worm is also capable of locomoting in a liquid medium, using a faster oscillation and different body shape. This behaviour is often referred to as thrashing or swimming.

The worm's locomotion is controlled by a small, known subset of its nervous system [8], and manipulations at the genetic or neuronal level allow insight into its inner workings. The apparent modularity of this subsystem, along with its easily observable output, make the locomotion nervous system a particularly appealing subject for modelling work.

Various models of *C. elegans* locomotion (specifically crawling) have already been developed [3–7,9,10]. Nonetheless the system is still only partially understood and remains of significant interest to modellers and experimentalists [11–15].

One fundamental unresolved question is whether the rhythmic motor control of forward locomotion relies on a central pattern generator (CPG) circuit or on sensory feedback. The conventional wisdom (supported by all evidence to date) is that all rhythmic motor behaviours across the animal kingdom are produced by CPGs, but such a CPG has been elusive in the *C. elegans* locomotion circuit [4,9]. Thus, some models [4,6] propose a mechanism whereby undulations are activated by stretch receptors that provide sensory feedback from body posture, with no intrinsic neuronal oscillator. One possible issue with regard to any locomotion model of the worm is the relatively sparse modelling work on the body wall muscles.

In particular, it is not known which components of the locomotion subsystem are actively involved in generating and shaping locomotion. The candidates are the interneurons, ventral cord motorneurons, body wall muscles and the *C. elegans* body itself. Putting aside the possible contribution of the body (but see [4,6,7,9]), the two alternatives are either that the patterned activity of the motor neurons activates the muscles which then act as actuators to deliver the mechanical contractions, or, perhaps more interestingly, that in addition to neuronal activity, the muscles themselves are capable of generating oscillatory dynamics and/or of propagating such signals down the length of the worm. The former holds in most studied motor systems: the neural circuit generates a patterned output, and the muscles serve as actuators of that output. Interestingly, this does not appear to be the case in *Ascaris lumbricoides* [6,16] – a much larger but closely related nematode whose nervous system is structurally very similar to that of *C. elegans*.

In *Ascaris*, the body wall muscles are electrically coupled by gap junctions and appear to form a functional syncytium which produces spontaneous myogenic activity: voltage spikes superimposed on slow depolarisations, which propagate independently of the nervous system [16]. From this perspective, it may not be surprising if *C. elegans* muscles had a similar pattern generating (or pattern modulating) role in locomotion.

In the absence of a direct answer to this question, one may turn to behavioural evidence from locomotion-defective (or so called uncoordinated) mutant strains of the worm. Particularly instructive are mutations that might disrupt electrical signal flow between muscles. There are two known gap junction genes in *C. elegans* namely unc-7 and unc-9, mutations of which result in virtually identical phenotypes [17] where locomotion is severely impaired. Both are widely expressed, but only unc-9 is expressed in muscles. Liu et al. have shown that worms treated with unc-9 RNA interference (RNAi) to suppress unc-9 gene expression exhibit substantially reduced locomotion velocities [18]. The authors suggest that this effect should be attributed specifically

to the reduction in gap junction coupling between body wall muscles. Signal propagation through body wall muscles via strong gap junction coupling was also used as the basis of a recent locomotion model [10].

2.2. *Anatomy of body wall musculature*

The body wall muscles of *C. elegans* are divided into four quadrants (ventral left, ventral right, dorsal left and dorsal right) each of which consists of 23 or 24 trapezoidal cells, arranged in two staggered rows (see Fig. 1 in Ref. [18]). When it locomotes, the worm lies on its side, with the pairs of ventral and dorsal muscle quadrants contracting in unison. Gap junctions couple cells within each quadrant, as well as between quadrants (ventral left with ventral right, and dorsal left with dorsal right). Within a quadrant, gap junctions are found between each muscle cell and the two overlapping cells from the other row [18].

Nematode muscles are unusual in that they extend thin, non-contractile processes to the motor neurons in the nerve cord, where they receive their neuromuscular input. The gap junctions which couple cells from the two ventral (or dorsal) quadrants are found on these muscle arms, where they meet at the nerve cord. Each muscle typically has three to five arms [19].

2.3. *Typical effects of diffusive coupling*

Gap junctions are found in a range of organs and cell types in vertebrates as well as invertebrate species and are very common in excitable tissue (e.g., heart muscle, pancreas, and the nervous system). Many gap junctions have fixed conductance and act as resistive elements. The current flowing through such a resistor would be proportional to the voltage drop across it, or the potential difference between the two coupled cells, j and k: $I_{j,k} = G\,(V_k - V_j)$ where G denotes a constant conductance (or inverse resistance). In *C. elegans*, it appears that the conductance of some gap junctions is itself a function of the potential difference between the coupled cells. Nonetheless, for the purposes of this introduction, suffice it to consider whether the coupling is relatively 'weak' or 'strong', neglecting any functional dependence of the conductance.

If coupling is sufficiently strong, the coupled elements will fully synchronise. Therefore the more interesting cases are those of weak and intermediate coupling. Weakly coupled limit cycle oscillators have been the subject of much theoretical investigation [20–22]. Typically, the frequencies of the oscillators are pulled towards each other, and full or partial entrainment may result, depending on the difference in natural frequency and the strength of the coupling. In certain situations unexpected behaviour can result, such as antiphase oscillation [23], bursting [24] and even quenching [25].

Coupling between non-oscillating elements has received less attention, but here one would expect two main effects. First, gap junctions will allow diffusive currents to diminish potential differences between coupled cells. In addition, the input impedance of the cells will be affected altering their frequency response [26].

3. Methods

The anatomy of the body wall muscles was described in Section 2.2. To represent a single cell, with muscle arms, we developed a compartmental conductance based model, with one compartment for the cell body and ten compartments for each muscle arm. All active currents are included in the main compartment, while the arms are modelled as passive cables.

To extend our model to an entire quadrant, the structure was slightly simplified. In the work that follows, we have reduced each muscle quadrant to a chain of identical cells with nearest neighbour coupling, which is a valid simplification given the pattern of gap junction connectivity.

3.1. *Electrical properties of the muscle body*

We began by developing a conductance based model of the muscle body. The model contains three active currents [27,28]: fast and slow potassium currents (I_{Kf} and I_{Ks}) and a calcium current (I_{Ca}) that exhibits inactivation on both fast and slow timescales, mediated by Ca^{2+} and voltage respectively. We also include a standard leak conductance I_L. A circuit diagram of the complete model is shown in Figure 1. The membrane potential for the i^{th} muscle in the chain is therefore given by

$$C\frac{dV_i}{dt} = -\Sigma I_{\text{ion}} + I_{\text{in}} + I_{i-1,i} + I_{i+1,i}$$
$$\Sigma I_{\text{ion}} = I_{Ks} + I_{Kf} + I_{Ca} + I_L\,,$$

where I_{in} is the input current from the muscle arms (see Section 3.2) and $I_{j,k}$ are gap junction currents (see Section 2.3). The membrane currents are given by

$$\begin{aligned} I_{Ks} &= g_{Ks} n (V - V_{Ks}) \\ I_{Kf} &= g_{Kf} p^4 q (V - V_{Kf}) \\ I_{Ca} &= g_{Ca} e^2 f (1 + (h-1)\alpha_{Ca})(V - V_{Ca}) \\ I_L &= g_L (V - V_L)\,, \end{aligned}$$

with activation variables e, n, p, and inactivation variables f, h, q. Gating kinetics are given in terms of a generic variable x

$$\frac{dx}{dt} = \frac{x_\infty(V, V_{\text{half}(x)}, k_{(x)}) - x}{\tau_x}$$

with a steady state given by

$$x_\infty(X, X_{\text{half}}, k) = \frac{1}{1 + \exp\left[\frac{X_{\text{half}} - X}{k}\right]}\,,$$

and the calcium mediated inactivation is given by

$$h = x_\infty([Ca^{2+}]_i, Ca_{\text{half}(h)}, k_{(h)}).$$

In order to find values for the 29 parameters of this model we simulated voltage clamp and current clamp traces of the model, fitting the parameters to corresponding whole cell recordings of body wall muscle cells of acutely dissected worms [28]. We similarly fit the steady state I-V curves for I_K and I_{Ca} [27,28]. Parameters for which values were reported in the literature were limited to a range close to the reported values. Fits were obtained by an evolutionary algorithm (differential evolution [29]). The parameters obtained are given in Appendix A. Note that the value of $C = 30\,pF$ was not evolved, but was taken from [18] and used for compatibility with coupling parameters. All simulations were run with a 4^{th} order Runge-Kutta method with a time step of $0.1\,ms$.

3.2. *Muscle arms*

The muscles arms are modelled as passive cables, each characterised by membrane capacitance (c_m), membrane resistance (r_m) and longitudinal resistance (r_l) (see Figure 1). We used $N = 10$ discrete compartments for each arm, with five arms per muscle. The membrane potential of each arm compartment evolves according to

$$c_m \frac{dv_n}{dt} = I_{\text{in}_n} - I_{\text{out}_n} - I_{m_n} \;\text{ for }\; n = 1 : N,$$

where I_{in_n} is the current flowing into the n^{th} compartment, I_{out_n} is the current flowing out of the n^{th} compartment and I_{m_n} is the current leaking through the cell membrane, according to

$$I_{m_n} = \frac{v_n - V_L}{r_m} \;\text{ for }\; n = 1 : N.$$

The current flowing out of compartment n into compartment $n+1$ is

$$\begin{aligned} I_{\text{out}_n} &= \frac{v_n - v_{n+1}}{r_l} \;\text{ for }\; n = 1 : N-1 \\ I_{\text{out}_N} &= \frac{v_N - V}{r_l}\,, \end{aligned}$$

where V is the membrane potential of the muscle body. With the exception of the first compartment, the current that flows out of one compartment must flow into the next, so

$$I_{\text{in}_n} = -I_{\text{out}_{n-1}} \;\text{ for }\; n = 2 : N.$$

For two coupled muscles (whether on the dorsal or ventral side), the first compartment of arms on the right (left) muscle quadrant have

$$I_{\text{in}_1} = I_{\text{NMJ}} \pm I_{R,L},$$

where I_{NMJ} is the neuromuscular junction (NMJ) input, and $I_{R,L}$ is the inter-quadrant gap junction current described in Section 3.3. Finally, the total current flowing into the muscle body is the sum of currents flowing out of each of the five arms

$$I_{\text{in}} = -\Sigma I_{\text{out}_N}\,.$$

Since no data on the electrical properties of the arms could be found, the cable parameters were based on estimates of the specific capacitance (C_m) and resistance (R_m) of the membrane, and the specific resistance of the cytoplasm (R_l), scaled by the arm dimensions. This is described in more detail, along with a table of the parameters, in Appendix A.

3.3. *Coupling*

The inter-muscular gap junctions are characterised in [18]. Intra-quadrant gap junction conductance was found to be a function of the potential difference across the junction. Coupling between quadrants was reported to have no voltage dependence (and a significantly smaller conductance). The intra-quadrant gap junction current introduced in Section 3.1 is given by

$$I_{j,k} = G_{ss}(V_j - V_k)(V_j - V_k),$$

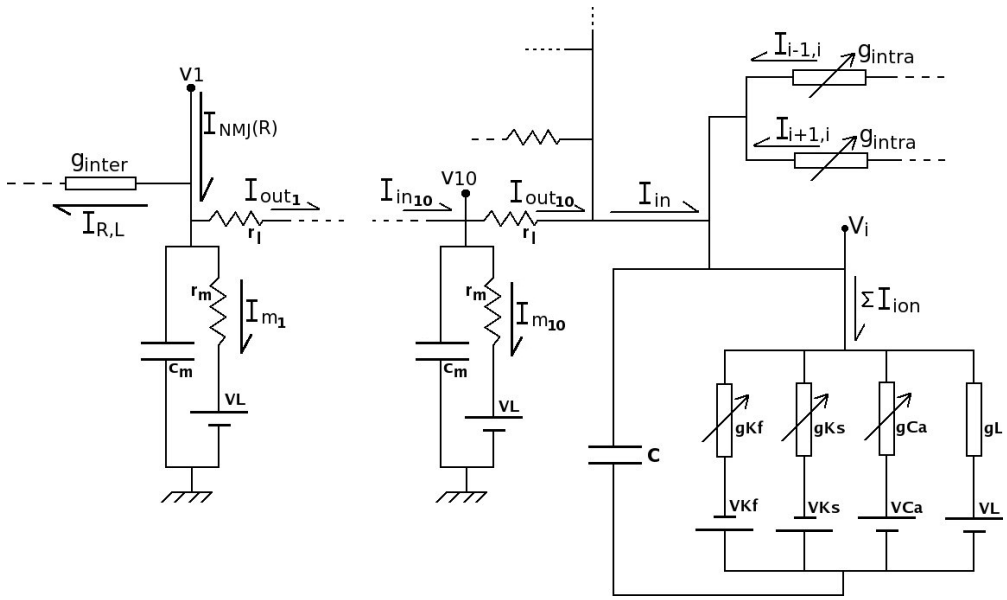

Fig. 1. Equivalent circuit diagram of the muscle model showing currents, voltages and parameters of the muscle body (bottom right of figure), muscle arms (with two of ten compartments of one arm shown and remaining arms appearing in parallel) and coupling. All labels correspond to those in the text.

where

$$G_{ss}(\Delta V) = g_{\text{intra}}\left[\frac{1-\Gamma_{\min}}{1+\exp(A(|\Delta V|-V_0))}+\Gamma_{\min}\right].$$

The inter-quadrant coupling from Section 3.2 is simply

$$I_{R,L} = g_{\text{inter}}(v_1(R) - v_1(L)),$$

where $v_1(R)$ is the potential of the first compartment of a right muscle arm and $v_1(L)$ is the potential of the first compartment of a left muscle arm.

3.4. *Current stimuli*

Inter-quadrant coupling occurs between cells that should be coactive (either on the ventral or dorsal side). To investigate whether these gap junctions could contribute to equalising input to left and right muscles, we stimulate the arms of the left and right muscle cells with sinusoidal currents of different amplitudes and monitor the resulting potential change in both left and right muscle bodies.

Intra-quadrant coupling is different, as it occurs between cells which would be expected to have slightly different input. The locomotion waveform of a crawling worm is periodic in time, with a frequency of about $0.5\,Hz$. It is also periodic in space, with a wavelength of approximately $\frac{2}{3}$ of the body length on agar. Given 24 cells in a muscle quadrant, a single wavelength should span $\frac{2}{3}24$ muscle cells. Therefore the inputs to adjacent muscles should be phase shifted by approximately $\frac{2\pi}{\frac{2}{3}24} = \frac{\pi}{8}$. It has been shown that the related nematode *Ascaris* has non-spiking neurons and graded synaptic transmission [30]. We will make the common assumption that *C. elegans* motorneurons share these properties. We therefore expect the current input to each muscle to be some smoothly varying function. The results from two such functions are shown in Section 4.3.2. Similar results were obtained for all other waveforms tested.

While this work will focus on crawling, for completeness we will also perform simulations using sinusoidal stimuli over a range of frequencies and phase lags. This range includes values typical of crawling and swimming. When swimming the worm oscillates with a frequency of about $2\,Hz$ and often exhibits a characteristic "C" shape. While it is hard to measure exactly, the spatial wavelength of the body wave for swimming is approximately twice the body length, with only half a wave being visible at any one time. Therefore the inputs to adjacent muscles should be phase shifted by approximately $\frac{2\pi}{2\times 24} = \frac{\pi}{24}$.

3.5. *Signal-to-noise ratio*

Another potential effect of coupling is on signal-to-noise ratio (SNR). Synaptic vesicle release is a stochastic process, so neuromuscular currents are likely to have a random component. Rather than explicitly modelling vesicle release, we have used an approximation where input to each muscle consists of a periodic signal combined with additive white Gaussian (zero-mean) noise. The method used for estimating the SNR of a signal is described in Appendix B.

4. Results

4.1. *Behaviour of the single cell model*

We wanted our single cell model to reproduce the electrophysiological data of a body wall muscle cell under voltage- and current-clamp conditions. Figure 2 shows the experimental voltage- and current-clamp traces [28] along with corresponding traces produced by simulation of our model with matching inputs. Likewise Figure 3 shows I-V curves for I_K and I_{Ca} (recorded and simulated). The model output is quantitatively very similar to the experimental data.

Having verified the validity of our model under these controlled conditions, we went on to investigate whether the cell could produce action potentials. In contrast to *Ascaris* body wall muscles [31], our model muscles are incapable of sustained spiking, either spontaneously or in response to current injection. Even when the fitness function for the parameter optimisation was altered to specifically reward oscillatory behaviour, sustained spiking could not be achieved for realistic values of g_{Ca}. The non-spiking nature of the model is consistent with the recently observed behaviour of the muscles in semi-intact worms [32]. The steady state I-V curve for an entire model muscle cell is shown in Figure 4. The voltage response diminishes as current increases, giving rise to a concave I-V relationship.

Our model predicts that *C. elegans* body wall muscles respond to stimuli with graded potential changes. The model reproduces the observed electrophysiological characteristics of voltage and current clamped body wall muscle cells well [28], giving us an excellent starting point for investigating the effect of inter-muscular coupling.

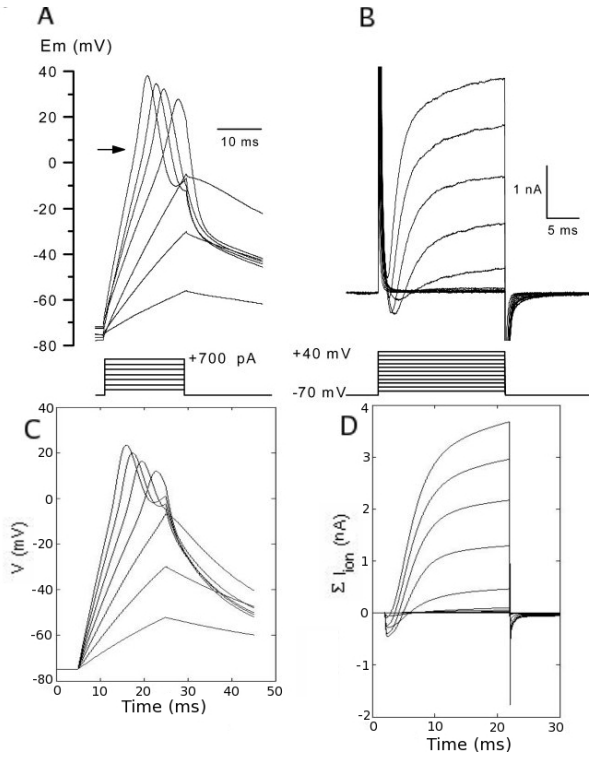

Fig. 2. Whole cell current (A) and voltage (B) clamp traces from body wall muscle cells reproduced with permission from [28], with stimulus protocols shown below the traces. The response of our model muscle cells to identical stimuli are shown in (C) and (D).

4.2. *Coupling between quadrants*

Given that inter-quadrant coupling occurs between cells which are expected to be coactive, we sought to determine whether these gap junctions could help to synchronise activity in the left/right cell pairs. While inter-quadrant coupling has been reported to have very low conductance ($75\,pS$ versus $370\,pS$ for intra-quadrant coupling) [18], it is plausible that the location of these junctions on the tiny muscle arms might increase their significance.

Although the cell pairs in question are innervated by the same neurons, properties of the individual neuromuscular junctions could cause the cells to receive slightly variable input. This could take the form of an amplitude difference or a time delay in the inputs. The effect of coupling when inputs to adjacent cells are phase shifted by an amount ϕ is dealt with in Section 4.3.2, for the stronger intra-quadrant gap junctions. Here we consider the case where the cells receive input of different amplitude.

We simulate two cells (each with five arms as

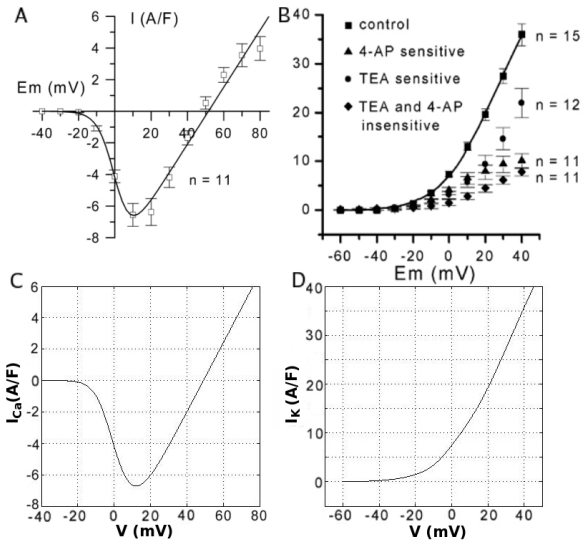

Fig. 3. Current-voltage relationships for the peak calcium (A) and steady state potassium (B) currents taken with permission from [28] and [27] respectively. Currents are shown normalised by cell capacitance. In (B), the relevant curve is the one labelled control. The corresponding relationships produced by our model are shown in (C) and (D).

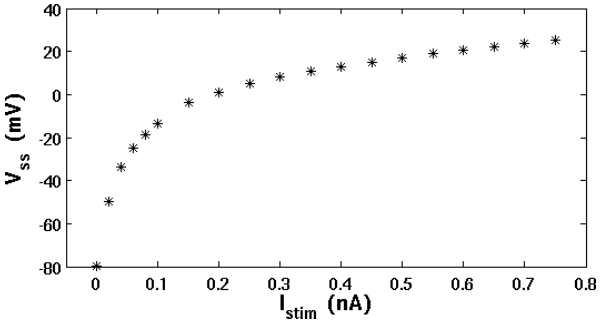

Fig. 4. Whole cell I-V curve for a model muscle cell. The cell was held at -70mV by injecting hyperpolarising current and then stimulated with 400 ms depolarising current steps. The membrane potential at the end of the stimulus was recorded.

described in Section 3.2) and stimulated the arms of both muscles with depolarising current. One cell (left) receives the full stimulus with amplitude A, while the other (right) receives input A' (as shown schematically in Figure 5 A) attenuated by α such that $A' = \alpha A$. For each α we run the simulation with and without gap junction coupling and in each case calculate the difference in the membrane potential between the left and right cells as an average absolute deviation (denoted δ)

$$\delta = \overline{|V_{left} - V_{right}|}\,.$$

The effect of the coupling ϵ is then obtained by comparing δ between coupled and uncoupled muscle cell pairs

$$\epsilon = \frac{\delta_{uncoupled} - \delta_{coupled}}{\delta_{uncoupled}}\,.$$

The results are shown in Figure 5 B. As can be seen, the percent change induced by the gap junctional coupling increases with the level of attenuation. This is not surprising, since depolarisation of the cells causes their total membrane conductance to increase (see concave relationship in Figure 4), thereby making the relative contribution of gap junction currents smaller by comparison. However, note that while the stimulated muscle responds strongly, the potential of the coupled cell is only weakly affected (under 3% even for the maximal attenuation). Finally, for this most extreme (and unrealistic) case of 100% attenuation, we also show the membrane potentials in the body compartments of both cells (Figure 6). When the potential of each compartment was plotted (not shown), we observed virtually no decrement in voltage down the arms, consistent with experimental observations [33].

It seems clear from these simulations that inter-quadrant coupling is too weak to contribute any significant current flow between left and right coupled muscle cells.

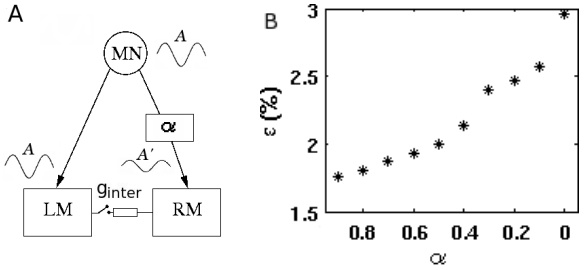

Fig. 5. (A) Model structure used to investigate the effect of gap junctional coupling between left and right quadrant muscle cells that are innervated by the same set of motorneurons (MN). The left muscle cell (LM) receives the full stimulus of amplitude A, while the right cell (RM) receives an attenuated signal of amplitude $A' = \alpha A$. Simulations are performed with and without gap junctional coupling g_{inter}. (B) The percent change (ϵ) in the voltage difference between the left and right cells increases with increasing attenuation.

4.3. *Coupling within quadrants*

We now want to determine the role of the stronger intra-quadrant coupling in locomotion. There are several possible avenues which must be investigated and we address these in turn.

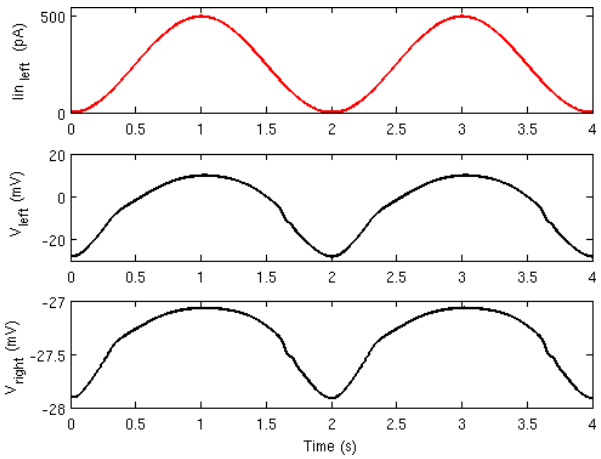

Fig. 6. Effect of inter-quadrant coupling in the extreme (unrealistic) case of 100% attenuation. The left muscle arms are stimulated by a sinusoidal current with peak amplitude of $500pA$ while the right muscle arms are unstimulated. This leads to significant depolarisation of the left muscle (middle), which in turn causes current to flow through the gap junction into the right muscle arms. The resulting depolarisation of the right muscle body is just under 1mV (bottom).

4.3.1. *Propagating activity*

A key question is whether the combination of active, excitatory currents and electrical coupling might allow regenerative propagation of activity down the chain of muscles, as reported in *Ascaris* [16]. Not only does the absence of spikes make this unlikely, but we show that the coupling is also insufficiently strong. Experiments with our model suggest that an increase of four fold in g_{Ca} (required to allow spiking) and about six fold in g_{intra} would be required to allow regenerative propagation (not shown).

Even if true regenerative propagation is not possible, stimulation at one end of the chain of muscles could still propagate significantly, albeit with attenuation. To investigate to what degree this occurs, we simulated a chain of cells and stimulated the first cell with a strong ($250pA$ for $500ms$) current pulse and observed the resulting depolarisation in all cells in the chain. As shown in Figure 7 the first (stimulated) cell is strongly depolarised. There is a peak depolarisation of only about $2mV$ in the second cell and almost no signal propagates to the third cell (peak depolarisation $< 0.5mV$).

Our model suggests that for the reported conductance values [18,28], signal propagation through a muscle quadrant can be ruled out as a mechanism for generating the locomotion waveform.

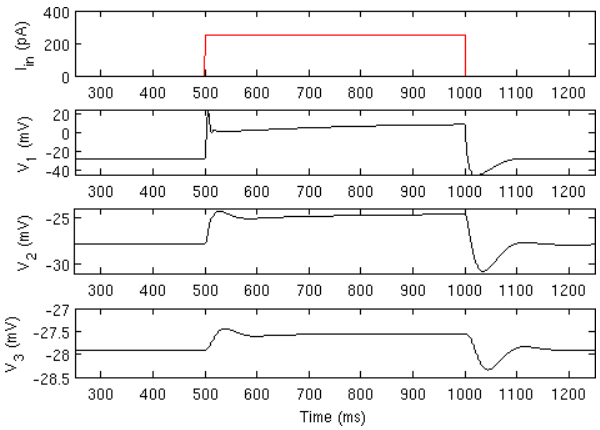

Fig. 7. Gap junction coupling is too weak to significantly propagate activity. We simulate a muscle quadrant (only three cells shown) and stimulate the first with a strong current pulse ($250pA$ for $500ms$). This causes a large ($> 40mV$) depolarisation of the first cell (V_1), and small ($< 3mV$) depolarisation of the second (V_2). By the third cell the depolarisation is insignificant ($< 0.5mV$).

4.3.2. *Waveform modulation*

Next, we asked whether the coupling within muscle quadrants could be involved in modulating the waveforms of muscle activation produced by neural inputs. We began by simulating a chain of 24 muscle cells with nearest neighbour coupling, as described in Sections 3.1 and 3.3. Current stimuli were applied as discussed in Section 3.4. Simulations were repeated with $g_{\text{intra}} = 0$ so that the resulting waveforms could be compared for the coupled and uncoupled cases.

Figure 8 A and B show the results of these simulations for two different input current waveforms. Traces are shown for two representative neighbouring cells from near the middle of the chain. For all the input waveforms tested, removing the coupling led to a barely noticeable change in the membrane potential traces. Looking closely, one can see that the difference in coupled and uncoupled potential becomes smaller as the cells are depolarised. This is not surprising, since depolarisation of the cells causes their total membrane conductance to increase, thereby making the relative contribution of g_{intra} smaller.

For any input waveform without discontinuities, the potential difference across the gap junctions will increase as the phase lag increases over the range 0 to π. To investigate the dependence of coupling significance on both frequency (F) and phase lag (ϕ), we performed simulations using sinusoidal input currents over a range of frequencies and phase

lags, chosen to completely cover the range of locomotion behaviours exhibited by the worm. To quantify the effect of the coupling for each F, ϕ pair, we began by calculating the magnitude of the voltage difference for the coupled and uncoupled muscle potential waveforms at each time step. In Figure 9 we show both the mean and the peak values of this difference, taken over two periods of the input wave. As can be seen, the frequency of the input wave has little effect on the significance of coupling, while increasing the phase lag does have a large effect. Since the phase lag is smaller for swimming than for crawling, an investigation of the latter is better suited to revealing possible coupling effects.

The effect of coupling on $[Ca^{2+}]_i$ levels is generally even smaller than the effect on membrane potential. This is because changes in V below the threshold for I_{Ca} have no effect on $[Ca^{2+}]_i$. As a final test we stimulated the muscles with an input waveform specifically designed to maximise the effect on $[Ca^{2+}]_i$, a square wave input that (though unrealistic) maximises the potential difference across the gap junctions, which in turn maximises the resulting current. We also added a depolarising bias current to give the cells a new resting potential of around $-10\,mV$ where the gradient in the I-V curve for I_{Ca} starts to become steep (see Figure 3). As can be seen in Figure 10, the effect of coupling on $[Ca^{2+}]_i$ is indeed larger in this case, peaking at about 15% for a crawling waveform. However this peak is a brief transient and is followed by a negative trough of similar amplitude. Thus the average effect on $[Ca^{2+}]_i$ is small and would be unlikely to result in a significant behavioural change.

Overall, the simulations we performed strongly suggest that the intra-quadrant coupling has too small an effect on the activation of body wall muscles to result in any observable change in the worm's locomotion.

4.3.3. *Role of coupling in noise reduction*

In all our simulations so far, we have been assuming that the neuromuscular inputs are clean signals untarnished by noise. However, since the release of neurotransmitter at chemical synapses is a stochastic process, we expect that the real neuromuscular inputs would exhibit fluctuations. This then begs the question whether the coupling between muscles could have an effect on signal-to-noise ratio (SNR). Electrically, the cell can be approximated as a capacitance in parallel with a resistance (see Fig. 1) which makes the cell membrane behave much like a simple low-pass filter with time constant $\tau = \dfrac{C_{\text{mem}}}{G_{\text{mem}}}$. Since G_{mem} is dynamic τ will also be. Coupling will change the effective impedance of the cells, thereby changing the properties of this filter.

To determine the extent to which this occurs, we performed simulations with a current stimulus consisting of a periodic signal with an additive noise component (as described in Section 3.5). Simulations were run both with and without coupling, for various values of noise variance σ. We then estimated the SNR of the input current and of the resulting V and $[Ca^{2+}]_i$ waveforms (as described in Appendix B). In the absence of coupling, the low-pass characteristics of the cell leads to a significant improvement in the SNR of the membrane potential over that of the input current signal. The additional low-pass effect of $[Ca^{2+}]_i$ leads to an even better SNR in the calcium waveform. When coupling is added, however, there is only a very small further improvement in SNR, as illustrated in Figure 11. We can therefore conclude that the impedance of the individual muscle membrane is by far the dominant factor in determining the frequency response of the muscle quadrant as a whole.

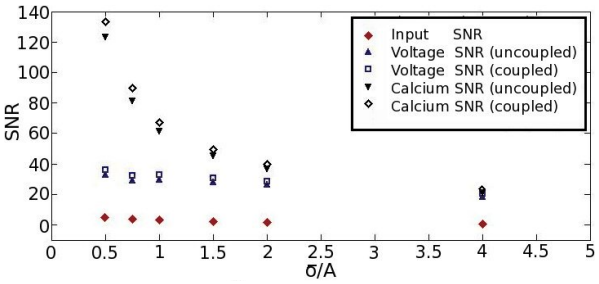

Fig. 11. Two stages of low-pass filtering occur in the muscles, having a large effect on SNR. The first stage has its effect on the membrane potential, and the second on the internal calcium concentration. Coupling results in a small further improvement due to a small change in the effective input impedance.

5. Discussion

We have presented a first detailed electrophysiological model of *C. elegans* body wall muscles. We use this model to test several hypotheses about the possible role of these muscle cells in the locomotion of the worm. Model parameters were found such that the membrane properties of the cell bodies match experimental recordings. A possible caveat on those

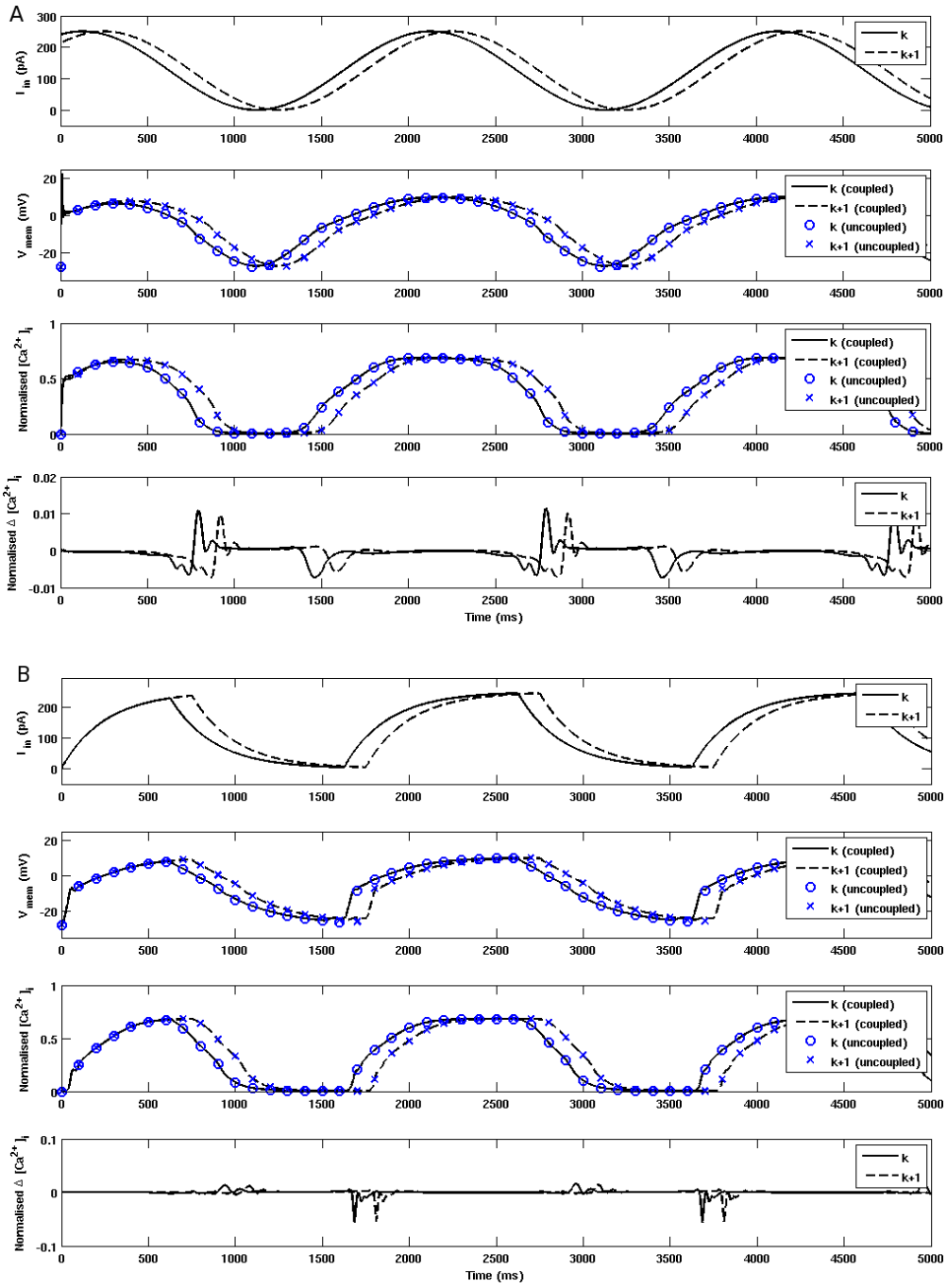

Fig. 8. The effects of intra-quadrant coupling for two possible crawling waveforms. Inputs are (A) sinusoidal and (B) "sawtooth" (similar to the outputs of the neural model in Refs. [4,9]), with frequency of 0.5Hz and a phase shift of $\frac{\pi}{8}$ between adjacent cells. In each case the simulations were performed with a chain of 24 coupled cells. Each plot shows (from top) the input current, membrane potential with and without coupling, normalised internal calcium concentration ($[Ca^{2+}]_i / \max[Ca^{2+}]_i$) with and without coupling, and the difference between the coupled and uncoupled calcium concentrations ($\Delta[Ca^{2+}]_i = ([Ca^{2+}]_{i,\text{coupled}} - [Ca^{2+}]_{i,\text{uncoupled}}) / \max[Ca^{2+}]_i$) for two representative (neighbouring) cells from near the middle of the chain. Note the nearly identical waveforms with and without coupling.

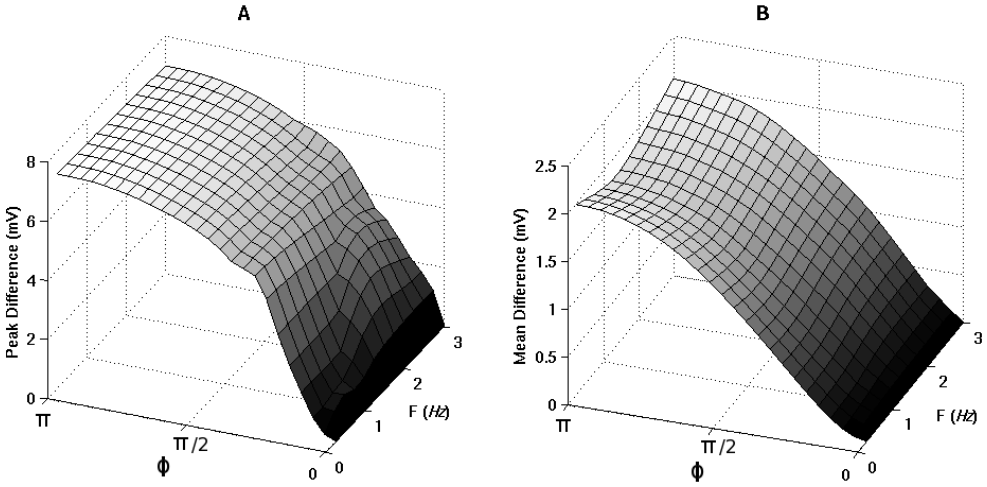

Fig. 9. The significance of muscle coupling depends strongly on the phase lag (ϕ) and weakly on the frequency (F) of the sinusoidal input waveform. The effect is quantified by the peak (A) and mean (B) value of the difference between the muscle potential traces in the coupled and uncoupled cases. Phase lags used range from 0 to π in steps of $\pi/24$.

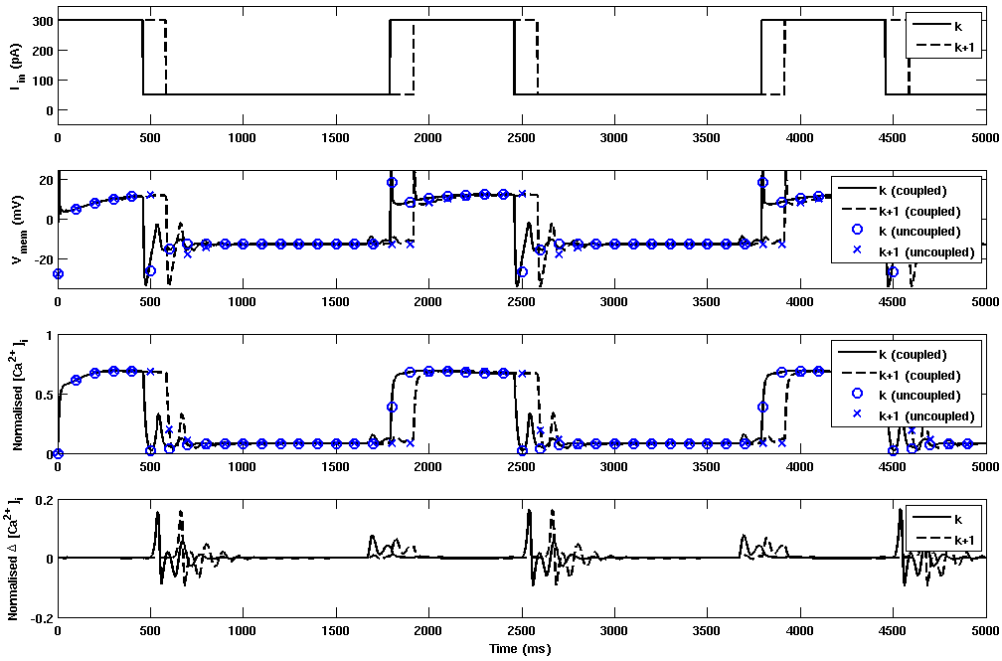

Fig. 10. Effect of intra-quadrant coupling in the most extreme case of square wave input with a depolarising bias, which increases the sensitivity of $[Ca^{2+}]_i$ to potential changes. Panels show (from top) the input current, membrane potential with and without coupling, normalised internal calcium concentration with and without coupling, and the difference between the coupled and uncoupled calcium concentrations, as in Figure 8.

parameters is the lack of relevant *in vivo* data to date. Nonetheless, the model presented is likely to provide a valid first approximation of muscle dynamics in a behaving worm.

All of the results presented here strongly suggest that in fact, *C. elegans* muscles are most likely to act only as actuators, and are not capable of communicating signals in a sufficiently effective manner, either to participate in pattern generation, or to propagate electrical oscillations.

5.1. *Single cell dynamics*

First, we rule out the possibility of sustained calcium action potentials for parameters anywhere within the ballpark of the model we have presented. The fact that conductances would have to increase many fold to yield any oscillations in the model cells suggests that such behaviour is unlikely *in vivo*. This is an interesting result and contrasts with reported results for the related nematode worm *Ascaris lumbricoides* but appears to be consistent with recent experiments on *C. elegans* body wall muscles [32]. That said, the absence of action potentials in body wall muscles does not, in itself, preclude a possible role of these muscle cells in rhythmic pattern generation. (Indeed, there are no known action potentials in the interneurons and motor neurons of the locomotion system either.)

Another question is what role the muscles may have in shaping locomotion. Figure 8 shows that the waveform of electrical activity in muscles closely follows the waveform of the input. This holds true both with and without inter-muscular coupling. The muscles therefore seem to effectively be actuators. Possibly interesting properties of the muscle cells are the concave I-V relationship shown in Figure 4 (which could endow them with an extended dynamic range) and their capability for some (limited) low-pass filtering. The extended dynamic range and low-pass characteristics should, if anything, improve robustness to changes in levels of neural activity and stochasticity of neurotransmitter release respectively.

5.2. *Muscle coupling*

To determine the possible roles of the body wall muscle coupling, first, in pattern generation, second, in the propagation of signals along the worm, and third, in waveform shaping, we present simulations of chains of coupled muscle cells (modelling a single quadrant of body wall muscles in the worm) and pairs of coupled muscle cells (modelling inter-quadrant coupling). In these simulations, the limiting factor is the strength of the gap junctional coupling. In fact, it appears that the reported conductance values are too low to support effective signal transmission between adjacent muscle cells, as our simulations suggest. While this initially seemed to perhaps be inconsistent with the unc-9 RNAi data of Liu et al. [18], a recent publication by the same group [34] strengthens our conclusion. In one experiment, mutant worms lacking unc-9 mediated gap junctions were reported to have this genetic defect selectively rescued in either neurons or muscles. This was done by expression of functional (wild-type) unc-9 under the control of promoters specific to neurons (P*rab*-3) or muscles (P*myo*-3) respectively. Selective rescue attempts in neurons "largely rescued the locomotion defect", while the selective rescue attempts in muscles "showed no obvious effect" [34].

5.3. *Muscle stretch receptors*

It has been suggested that *C. elegans* body wall muscle cells also possess so called stretch receptor channels, that depolarise the cell in response to bending or stretching of the body [35]. If so, in a rhythmically bending or undulating worm, the muscles may, in principle, have the capacity to respond to the alternating body posture actively (but still with graded potential changes) thus aiding and maintaining this oscillatory behaviour. Such a sensory-feedback mechanism mimics closely existing models of sensory feedback driving neuronal activation in the ventral cord [4,7,9]. However, if this were true, such a mechanism would operate effectively independently from any neurally generated oscillations, since the only points of contact between muscles and the nervous system (the neuromuscular junctions) only allow information flow in one direction – from the neurons to the muscles. Thus, to be interesting (i.e. to contribute significantly to pattern generation), muscles distributed along the body of the worm would need to coordinate their oscillations. Here we have demonstrated that the weakness of the gap junctional coupling precludes the communication of such signals along a chain of muscles.

5.4. *Relevance to locomotion models*

If the observed phenotypes of unc-9 mutant and RNAi treated worms cannot be explained in terms of muscle gap junctions, then it stands to reason that disruption of neuronal gap junctions must be involved. Gap junctions are quite prevalent in *C. elegans*, and are found throughout the nervous system. In the ventral cord neural circuit for locomotion, gap junctions are found primarily between interneurons and motorneurons, and between motorneurons of the same class [8].

Consistent with the known neural circuitry [8], several locomotion models [4,7,9,36] rely on what has been dubbed the "core circuit" [4,9] for forwards locomotion. In these models, the pair of forwards locomotion command interneurons (of class AVB) are gap junctionally coupled to motorneurons. The two primary forward locomotion motorneuron classes (VB and DB) also function as sensory neurons, detecting the degree of body bending using postulated stretch receptors. These three neuron classes, with mechanical feedback via the body, are sufficient to generate the antiphase oscillations for forward locomotion. Since there are no chemical synapses from AVB to the VB/DB class neurons, gap junctional coupling would appear to be crucial in generating locomotion. In Ref. [9] it is also predicted that the level of input from AVB modulates the speed of locomotion. It is generally assumed that a similar mechanism involving the AVA interneurons and VA/DA class motorneurons accounts for backward locomotion.

More recently an alternative model has been suggested [10] in which a central pattern generator (CPG) in the worm's head generates oscillations which propagate down the muscles through strong gap junctional coupling. Such a mechanism is appealing due to its similarity to what is thought to be the case in *Ascaris*. However our simulations indicate that muscles do not fire action potentials in response to neuromuscular input (consistent with Ref. [32]), and that muscle gap junctions are electrically negligible and cannot effectively propagate signals (consistent with Ref. [34]).

Ultimately, the task of modelling *C. elegans* locomotion combines an understanding of integrated contributions from the nervous system, muscles, physical body and environment of the worm. The realistic muscle model presented here complements existing models of the body and environment [5,36,37]. Thus, given a postulated or recorded pattern of motorneuron activities (and given appropriate interfaces between muscle potential and mechanical contraction [38]), it should be possible to solve the forward problem and infer the resulting dynamic body shapes of the locomoting worm. The apparently simple transfer function of the muscles that emerges from this paper makes the forward problem all the more tractable.

By contrast, the inverse problem of inferring neural activity patterns from body shapes (or even from patterns of muscle activations) is much harder, essentially due to its underdetermined nature. In other words the multiplicity of neuronal inputs into each muscle cell makes the inverse problem too difficult to tackle in the absence of additional constraints (or assumptions) on the neuronal model.

6. Conclusions

We have presented a biologically grounded model of body wall muscle cells and their gap junctional coupling in *C. elegans*. The model and simulations suggest that the neural circuit is the active component generating the rhythmic patterns of locomotion (though we shed no light on the neural mechanism of generating such patterns – whether via a central pattern generating circuit, or via sensory feedback from stretch receptor channels).

Also, we have shown that the phenotypes of unc-7 or unc-9 mutation, or of unc-9 RNAi, cannot be explained by our model in terms of muscle gap junctions. One may therefore speculate as to which gap junctions (elsewhere in the locomotion system) may account for the reduced velocity observed in these mutant and RNAi treated worms. A likely candidate is the gap junctional coupling between the forward locomotion command interneurons AVB and forward locomotion motor neurons of classes VB and DB. Interestingly, models of the neural control of forward locomotion [4,9] have also suggested that modulation of command input into these motor neurons can modulate locomotion velocity [9].

This work was funded by the EPSRC, grant EP/C011961. NC was funded by the EPSCR, grant EP/C011953. Thanks to Stefano Berri for movies of worms and behavioural data, and to Bruno Allard and Zhao-Wen Wang for giving such helpful answers to my questions.

Appendix A. Model parameters

A.1. *Parameters for the muscle body*

Due to the complexity of the fitness landscape for these parameters, multiple iterations of the evolutionary algorithm produced similar, but non-identical parameter sets. One such set (the one used for the simulations in this paper) is presented in Table A.1.

Param.	Value	Reported Val.	Param.	Value	Reported Val.
C_A	$72.3pF$	$\sim 75pF$ [28]	C_B	$30pF$	$29.6pF$ [18]
g_{Ks}	$436S/F$	$399S/F$ [27]	V_{Ks}	$-64.3mV$	$-67.9mV$ [27]
g_{Kf}	$400S/F$	$423S/F$ [27]	V_{Kf}	$-55.0mV$	$-47.0mV$[27]
g_{Ca}	$220S/F$	$199S/F$ [28]	V_{Ca}	$49.1mV$	$50.0mV$ [28]
g_L	$19.3S/F$	$22S/F$ [18]	V_L	$10.0mV$	n/a
αCa	0.283	n/a	ϕCa	$2.39 \cdot 10^{-6}$	n/a
$V_{0.5_n}$	$19.9mV$	n/a	k_n	$15.9mV$	n/a
$V_{0.5_p}$	$-8.1mV$	n/a	k_p	$7.4mV$	n/a
$V_{0.5_q}$	$-15.6mV$	n/a	k_q	$-10.0mV$	n/a
$V_{0.5_e}$	$-3.4mV$	n/a	k_e	$6.7mV$	n/a
$V_{0.5_f}$	$25.2mV$	n/a	k_f	$5.0mV$	n/a
$Ca_{0.5_h}$	$64.1 \cdot 10^{-9}$	n/a	k_h	$-10\mu M$	n/a
τ_n	$25.0ms$	n/a	τ_p	$2.3ms$	n/a
τ_q	$150ms$	n/a	τ_e	$0.10ms$	n/a
τ_f	$151ms$	n/a	τ_{Ca}	$11.6ms$	n/a

Table A.1
Parameters for the muscle body obtained by fits to experimental traces (see text for detail). Reported values are given where possible. The two values of C_A and C_B were used in our simulations for compatibility with voltage- and current-clamp data [27,28] and coupling parameters [18] respectively.

A.2. *Muscle arm parameters*

We began by estimating values for the specific capacitance (C_m) and resistance (R_m) of the membrane, and the specific resistance of the cytoplasm (R_l). Using the standard value of $C_m = 1\,\mu F/cm^2$, a cell with $C = 30\,pF$ (as in [18]) should have a surface area of $3 \times 10^{-3}\,mm^2$. The same cell was reported to have $G_{in} = 1/R_{in} = 666\,ps$, so $R_m = 45 \times 10^3\,\Omega\,cm^2$. Finally a standard value of $R_l = 100\,\Omega\,cm$ was chosen. Approximating each muscle arm as a cylinder with $l = 10\,\mu m$ and $r = 0.75\mu m$ (which we divide into ten compartments), we obtain:

$$c_m = C_m 2\pi r l$$
$$r_m = \frac{R_m}{2\pi r l}$$
$$r_l = \frac{R_l l}{\pi r^2}\,.$$

The resulting parameter values are given in Table A.2.

N	c_m	r_m	r_l
10	$47\,fF$	$950\,G\Omega$	$570\,k\Omega$

Table A.2
Muscle arm compartment parameters, obtained from estimates of the cell properties and dimensions (see text).

A.3. *Coupling parameters*

As a conservative choice of g_{intra}, we used the peak value reported in Ref. [18]. The value of g_{inter} is the reported value of $75\,pS$ divided evenly across the five arms of each muscle cell. The remaining parameters set the voltage dependence of the intra-quadrant coupling and were obtained by curve fitting to the experimental G/V curve in [18]. The parameters are given in Table A.2.

g_{intra}	g_{inter}	Γ_{min}	A	V_0
$370\,pS$	$15pS$	0.13	40	$60\,mV$

Table A.3
Intra- and inter-quadrant coupling parameters. g_{intra} and g_{inter} were reported [18]. The remaining parameters were obtained by curve fitting to Figure 2. B of Ref. [18].

Appendix B. Calculating signal-to-noise ratio

We use spectral methods to calculate the signal-to-noise ratio (SNR) in a model muscle cell, stimulated with a superposition of a sinusoidal wave and white Gaussian noise. The input signal we use has a period $T = \dfrac{2\pi}{\omega_{\text{in}}} = 2s$. Simulations were run for a total duration of $D = 8s$ with a time step of $\Delta t = 0.01ms$.

The SNR is estimated from the power spectrum density (PSD) of the muscle output. For a signal $x(t)$, the PSD is given by

$$\text{PSD}(\omega) = X(\omega)X^*(\omega)/N\,,$$

where $X(\omega)$ is the Fourier transform of the signal (calculated with a fast Fourier transform or FFT, with $N = 2^{19}$, and the asterisk denotes complex conjugation.

To estimate the SNR from the PSD, we must first specify what frequency range will be considered "signal". Ideally the input should appear in the frequency domain as a spike of zero width at $0.5\,Hz$. In reality the signals (particularly the "filtered" signals V_i and $[Ca^{2+}]_i$) will be smeared to some extent,

leading to a peak of nonzero width. Based on visual inspection of the PSD, we have assigned all components on the range 0-5 Hz to the signal, and from 5 Hz to 50 kHz to noise. While there will be some noise in the 0- 5Hz range, this represents only 0.1% of the total bandwidth, and will not significantly affect the results. Finally we obtain values for the signal power, P_{signal}, the noise power P_{noise} and the ratio SNR as follows

$$P_{\text{signal}} = \frac{1}{N}\Sigma_{-5Hz}^{5Hz}\text{PSD}(\omega)$$
$$P_{\text{noise}} = \frac{1}{N}\left[\Sigma_{5Hz}^{50kHz}\text{PSD}(\omega) + \Sigma_{-50kHz}^{-5Hz}\text{PSD}(\omega)\right]$$
$$\text{SNR} = \frac{P_{\text{signal}}}{P_{\text{noise}}}\,.$$

The SNR is then calculated for different values of the input noise variance.

References

[1] D. L. Riddle, T. Blumenthal, B. J. Meyer, J. R. Priess (Eds.), *C. elegans* II, 2nd Edition, Cold Spring Harbour Laboratory Press, New York, 1997.

[2] C. elegans Sequencing Consortium, Genome sequence of the nematode *C. elegans*: A platform for investigating biology, Science 282 (1998) 2012–2018.

[3] J. A. Bryden, A simulation model of the locomotion controllers for the nematode *Caenorhabditis elegans*, Master's thesis, University of Leeds (2003).

[4] J. A. Bryden, N. Cohen, A simulation model of the locomotion controllers for the nematode *Caenorhabditis elegans.*, in: S. Schaal, A. J. Ijspeert, A. Billard, S. Vijayakumar, J. Hallam, J. A. Meyer (Eds.), Proceedings of the eighth international conference on the simulation of adaptive behaviour, MIT Press / Bradford Books, 2004, pp. 183–192.

[5] M. Suzuki, T. Tsuji, H. Ohtake, A model of motor control of the nematode *C. elegans* with neuronal circuits, Artificial Intelligence in Medicine 35 (2005) 75–86.

[6] P. Erdös, E. Niebur, The neural basis of the locomotion of nematodes, Lecture Notes in Physics 368 (1990) 253–267.

[7] E. Niebur, P. Erdös, Theory of the locomotion of nematodes: Control of the somatic motor neurons by interneurons, Mathematical Biosciences 118 (1993) 51–82.

[8] J. G. White, E. Southgate, J. N. Thomson, S. Brenner, The structure of the nervous system of the nematode *Caenorhabditis elegans*, Philosophical Transactions of the Royal Society of London, Series B 314 (1986) 1–340.

[9] J. A. Bryden, N. Cohen, Neural control of *C. elegans* forward locomotion: The role of sensory feedback, submitted.

[10] J. Karbowski, G. Schindelman, C. J. Cronin, A. Seah, P. W. Sternberg, Systems level circuit model of *C. elegans* undulatory locomotion: mathematical modeling and molecular genetics, Journal of Computational Neuroscience, in press.

[11] B. L. Chen, D. H. Hall, D. B. Chklovskii, Wiring optimization can relate neuronal structure and function, Proceedings of the National Academy of Sciences USA 103 (2006) 4723–4728.

[12] J. Karbowski, C. J. Cronin, A. Seah, J. E. Mendel, D. Cleary, P. W. Sternberg, Conservation rules, their breakdown, and optimality in *Caenorhabditis* sinusoidal locomotion, Journal of Theoretical Biology 242 (2006) 652–669.

[13] J. Korta, D. A. Clark, C. V. Gabel, A. D. T. Samuel, Mechanosensation and mechanical load modulate the locomotory gait of swimming *C. elegans*, Journal of Experimental Biology 210 (2007) 2383–2389.

[14] S. J. Park, M. B. Goodman, B. L. Pruitt, Analysis of nematode mechanics by piezoresistive displacement clamp, PNAS 104 (2007) 17376–17381.

[15] G. J. Stephens, B. Johnson-Kerner, W. Bialek, W. S. Ryu, Dimensionality and dynamics in the behaviour of *C. elegans*, arXiv:0705.1548v1 [q-bio.IT] 11 May 2007.

[16] D. A. Weisblat, R. L. Russell, Propagation of electrical activity in the nerve cord and muscle syncytium of the nematode *Ascaris lumbricoides*, Journal of comparative Physiology 107 (1976) 293–307.

[17] P. Phelan, T. A. Starich, Innexins get into the gap, BioEssays 23 (2001) 388–396.

[18] Q. Liu, B. Chen, E. Gaier, J. Joshi, Z. W. Wang, Low conductance gap junctions mediate specific electrical coupling in body-wall muscle cells of *Caenorhabditis elegans*, Journal of Biological Chemistry 281 (2006) 7881–7889.

[19] S. J. Dixon, P. J. Roy, Muscle arm development in *Caenorhabditis elegans*, Development 132 (2005) 3079–3092.

[20] G. B. Ermentrout, n:m phase-locking of weakly coupled oscillators, Journal of Mathematical Biology 12 (1981) 327–342.

[21] B. D. Ermentrout, N. Kopell, Frequency plateaus in a chain of weakly coupled oscillators, I., SIAM Journal of Mathematical Analysis 15 (1984) 215–237.

[22] N. Kopell, G. B. Ermentrout, Symmetry and phaselocking in chains of weakly coupled oscillators, Communications on Pure and Applied Mathematics 39 (1986) 623–660.

[23] A. Sherman, J. Rinzel, Rhythmogenic effects of weak electrotonic coupling in neuronal models, Neurobiology 89 (1992) 2471–2474.

[24] A. K. Han, C. Kurrer, Y. Kuramoto, Dephasing and bursting in coupled neural oscillators, Physical Review Letters 75 (1995) 3190–3193.

[25] D. Ramana Reddy, A. Sen, G. L. Johnston, Time delay induced death in coupled limit cycle oscillators, Physical Review Letters 80 (1998) 5109–5112.

[26] N. Cohen, The development of spontaneous beating activity in cultured heart cells: from cells to networks, Ph.D. thesis, Israel Institute of Technology, Kislev, 5761, Haifa (December 2000).

[27] M. Jospin, M. C. Mariol, L. Segalat, B. Allard, Characterisation of K+ currents using an *in situ* patch clamp technique in body wall muscle cells from

Caenorhabditis elegans, Journal of Physiology 544.2 (2002) 373–384.

[28] M. Jospin, V. Jacquemond, M. C. Mariol, L. Segalat, B. Allard, The l-type voltage-dependent Ca2+ channel EGL-19 controls body wall muscle function in *Caenorhabditis elegans*, Journal of Cell Biology 159 (2002) 337–347.

[29] K. Price, R. Storn, Differential evolution, Dr. Dobb's Journal April (1997) 18–24.

[30] R. E. Davis, A. O. W. Stretton, Signalling properties of *Ascaris* motorneurons: Graded active responses, graded synaptic transmission, and tonic transmitter release, Journal of Neuroscience 9 (1989) 415–425.

[31] D. A. Weisblat, L. Byerly, R. L. Russel, Ionic mechanisms of electrical activity in somatic muscle of the nematode *Ascaris lumbricoides*, Journal of comparative Physiology 111 (1976) 93–113.

[32] Z. W. Wang, Personal Communication, reporting that no spiking was observed in recordings of *C. elegans* body wall muscles in acutely dissected preparations. (2007).

[33] J. E. Richmond, E. M. Jorgensen, One GABA and two acetylcholine receptors function at the *C. elegans* neuromuscular junction, Nature neuroscience 2 (1999) 791–797.

[34] B. Chen, Q. Liu, Q. Ge, J. Xie, Z. W. Wang, Unc-1 regulates gap junctions important to locomotion in *C. elegans*, Current Biology 17 (2007) 1334–1339.

[35] J. Liu, B. Schrank, R. H. Waterston, Interaction between a putative mechanosensory membrane channel and a collagen, Science 273 (1996) 361–364.

[36] J. H. Boyle, J. Bryden, N. Cohen, An integrated neuro-mechanical model of *C. elegans* forward locomotion, Proceedings of 14th International Conference on Neural Information Processing (ICONIP), in press.

[37] E. Niebur, P. Erdös, Theory of the locomotion of nematodes: Dynamics of undulatory progression on a surface, Biophysics Journal 60 (1991) 1132–1146.

[38] J. H. Boyle, N. Cohen, Mechanical properties of *C. elegans* body and environment, in preparation.